

Studies on characterization, telomerase inhibitory properties and G-quadruplex binding of η^6 -arene ruthenium complexes with 1,10-phenanthroline-derived ligands†

Dongdong Sun, Rong Zhang, Fang Yuan, Du Liu, Yanhui Zhou and Jie Liu*

Received 5th September 2011, Accepted 26th October 2011

DOI: 10.1039/c1dt11676b

Two arene ruthenium complexes $[\text{Ru}(\eta^6\text{-C}_6\text{H}_6)(\text{p-MOPIP})\text{Cl}]^+$ **1** and $[\text{Ru}(\eta^6\text{-C}_6\text{H}_6)(\text{p-CFPIP})\text{Cl}]^+$ **2**, where p-MOPIP = 2-(4-methoxyphenyl)-imidazo[4,5f][1,10] phenanthroline and p-CFPIP = 2-(4-trifluoromethylphenyl)-imidazo[4,5f][1,10] phenanthroline, were prepared and the interactions of these compounds with DNA oligomers 5'-G3(T2AG3)3-3'(HTG21) have been studied by UV-vis and circular dichroism (CD) spectroscopy, gel mobility shift assay, fluorescence resonance energy transfer (FRET) melting assay, polymerase chain reaction (PCR) stop assay and telomeric repeat amplification protocol (TRAP) assay. The results show that both complexes can induce the stabilization of quadruplex DNA but complex **1** is a better G-quadruplex binder than complex **2**. The two ruthenium complexes tested led to an inhibition of the enzyme telomerase and complex **1** was the significantly better inhibitor. A novel visual method has been developed for making a distinction between G-quadruplex DNA and double DNA by our Ru complexes binding hemin to form the hemin-G-quadruplex DNAzyme. Furthermore, *in vitro* cytotoxicity studies showed complex **1** exhibited quite potent antitumor activities and the greatest inhibitory selectivity against cancer cell lines.

Introduction

Telomeres are specific nucleoprotein structures essential for stability and complete replication of chromosomes.^{1,2} A key function of telomeres is to protect the termini of chromosomes from recombination and end-to-end fusion. Human telomeres are essential structures composed of telomeric DNA and telomere-binding proteins located at the ends of every human chromosome, and are composed of a repeated double-stranded [TTAGGGCCCTAA]_n sequence, except in the 3'-terminal region which consists of a single-stranded tandem [TTAGGG] repeated sequence over several hundred bases.³⁻⁶ In normal somatic cells, telomeres are shortened by 50–200 bases after each round of cell division, while reversal of this degradation by a specialized enzyme called telomerase increases cellular replicative capacity, leading to uncontrolled proliferation. However, telomerase is overexpressed in most tumor cells and telomerase activity is reported in 80–90% of tumors.⁶⁻¹⁰

Thus, the inhibition of telomerase activity by stabilizing G-quadruplex formation and detection of G-quadruplex DNA are important targets for developing new anticancer chemotherapy.¹¹⁻¹⁶ A number of small molecules have been reported to efficiently stabilize G-quadruplex DNA, and recently some metal complexes as G-quadruplex DNA stabilizers were

reported.¹⁷⁻²² The metal can play a major structural role in organizing the ligand(s) into an optimal structure for G-quadruplex DNA interaction. Also, the electropositive metal can in principle be positioned at the center of the guanine quartet, increasing electrostatic stabilization by substituting the cationic charge of the potassium or sodium that would normally occupy this site.

Ru^{II} complexes have prominent DNA-binding properties. For example, the complex $[\text{Ru}(\text{bpy})_2(\text{dppz})]^{2+}$ (dppz = dipyrdo [3,2-a:2',3'-c] phenazine) has been known as a DNA “light switch”. The complex can intercalate between the duplex DNA base pairs and stabilize the DNA.²³⁻²⁵ Rickling *et al.* have studied the action of the dinuclear $[(\text{tap})_2\text{Ru}(\text{tpac})\text{Ru}(\text{tap})_2]^{4+}$ complex (tap = 1,4,5,8-tetraazaphenanthrene, tpac = tetrapyrrodoacridine) with the d(TTAGGG)4 sequence. They found that the complex would be particularly interesting to damage these sequences by intramolecular photobridging of two or more G bases by using the metallic $[(\text{tap})_2\text{Ru}(\text{tpac})\text{Ru}(\text{tap})_2]^{4+}$. Indeed, this photoinduced bridging process would “freeze” the folded G-quadruplex conformation.²⁶ Arene ruthenium complexes have also been successfully used to stabilize telomeric quadruplex DNA, such as cationic octanuclear metalla-boxes $[\text{Ru}_8(\text{arene})_8(\mu\text{-tpp-H}_2)_2(\mu\text{-C}_6\text{H}_2\text{O}_4)_4]^{8+}$ (tpp-H₂ = 5,10,15,20-tetra(4-pyridyl)porphyrin, arene = C₆H₅Me and p-PrC₆H₄Me). The octacationic arene ruthenium metalla-boxes have shown promising quadruplex DNA stabilization and possessed a high degree of selectivity for quadruplex over duplex.^{27,28}

In this paper, we studied the interaction of two complexes $[\text{Ru}(\eta^6\text{-C}_6\text{H}_6)(\text{p-MOPIP})\text{Cl}]^+$ **1** and $[\text{Ru}(\eta^6\text{-C}_6\text{H}_6)(\text{p-CFPIP})\text{Cl}]^+$

Department of Chemistry, Jinan University, Guangzhou, 510632, P.R. China.
E-mail: tliuliu@jnu.edu.cn; Fax: +86-20-8522-1263

† Electronic supplementary information (ESI) available. See DOI: 10.1039/c1dt11676b

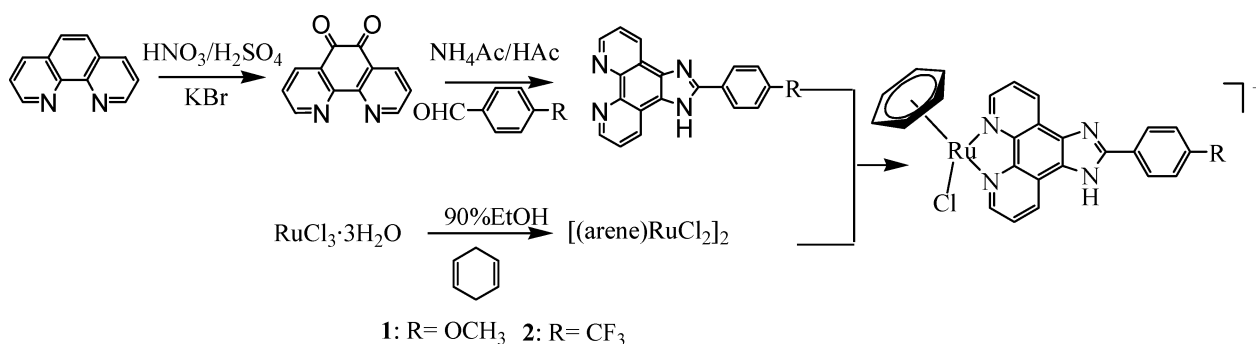


Fig. 1 Synthetic route to ruthenium(II) complexes.

2 with G-quadruplexes. The synthetic route and structures of **1** and **2** are shown in Fig. 1.

Experimental

Reagents and materials

All reagents and solvents were purchased commercially and used without further purification unless specifically noted, and Ultrapure MilliQ water (18.2 mX) was used in all experiments. DNA oligomers 5'-G3(T2AG3)3-3' (HTG21) and the complementary cytosine rich strand 5'-C3(TA2C3)3-3' (ssDNA) were purchased from Shanghai Sangon Biological Engineering Technology & Services (Shanghai, China) and used without further purification. Calf thymus (CT) DNA (highly polymerized) purchased from Sigma, was stored at 4 °C. Concentration of 5'-G3(T2AG3)3-3' (HTG21) and 5'-C3(TA2C3)3-3' (ssDNA) was determined by measuring the absorbance at 260 nm after melting. Single-strand extinction coefficients were calculated from mononucleotide data using a nearest-neighbour approximation.²⁹ The formation of intramolecular G-quadruplexes was carried out as follows: the oligonucleotide samples, dissolved in different buffers, were heated to 90 °C for 5 min, gently cooled to room temperature, and then incubated at 4 °C overnight. Buffer A: 10 mM Tris-HCl, pH = 7.4; Buffer B: 10 mM Tris-HCl, 100 mM NaCl, pH = 7.4; Buffer C: 10 mM Tris-HCl, 100 mM KCl, pH = 7.4. Solutions of CT DNA in the buffer 5 mM Tris HCl/50 mM NaCl in water gave a ratio of UV absorbance at 260 and 280 nm, A_{260}/A_{280} , of 1.9,³⁰ indicating that the DNA was sufficiently free of protein. Concentrated stock solutions of DNA (10 mM) were prepared in buffer and sonicated for 25 cycles, where each cycle lasted 30 s with 1 min intervals. The concentration of DNA in nucleotide phosphate (NP) was determined by UV absorbance at 260 nm after 1 : 100 dilutions. The extinction coefficient, $\epsilon_{260\text{ nm}}$, was taken as 6600 M⁻¹ cm⁻¹. Stock solutions were stored at 4 °C and used after no more than 4 days. Concentrated stock solutions of metal complexes were stored at 1 or 2 mM in DMSO, further dilution being made in the corresponding buffer to the required concentrations for all the experiments.

Physical measurements

Elemental analyses (C, H, and N) were carried out with a Perkin-Elmer 240 C elemental analyzer. ¹H NMR spectra were recorded on a Varian Mercury-plus 300 NMR spectrometer with DMSO-

d₆ as a solvent and SiMe₄ as an internal standard at 300 MHz at room temperature. Electrospray ionization mass spectrometry (ESI-MS) was recorded on a LQC system (Finnigan MAT, USA) using CH₃CN as a mobile phase. UV-Visible (UV-Vis) and emission spectra were recorded on Perkin-Elmer Lambda-850 spectrophotometer. Circular dichroism (CD) spectra were recorded on a Jasco J-810 spectropolarimeter.

Synthesis of ligands and complexes

The following were obtained from the stated chemical suppliers: Ruthenium^{III} chloride hydrate (Alfa Aesar), 1,10-phenanthroline, 4-(trifluoromethyl)benzaldehyde, 4-methoxybenzaldehyde and cyclohexa-1,4-diene (Sigma). The compounds of 1,10-phenanthroline-5,6-dione,³¹ [Ru(η⁶-C₆H₆)Cl₂]₂,^{32,33} p-MOPIP and p-CFPIP³⁴ were prepared and characterized according to methods in the literature.

Synthesis of [Ru(η⁶-C₆H₆)(p-MOPIP)Cl]²⁺ (**1**)

1 was synthesized in a similar manner to the complex [(arene)Ru(N ∩ N)Cl]⁺ (arene = C₆H₆, N ∩ N = phen).³⁵ Two equivalents (0.30 mmol) of the p-MOPIP ligand were added to a suspension of [Ru(η⁶-C₆H₆)Cl₂]₂ (0.15 mmol) in dichloromethane (40 mL). The mixture was stirred for 4 h at room temperature, during this time the colour changed from orange to ash-coloured. After evaporation to dryness, the residue was dissolved in water and the solution filtered and evaporated to dryness to give the product. The crude product was purified by column chromatography on a neutral alumina column with acetonitrile and toluene (2 : 1, v/v) as eluent. The mainly gray band was collected. The solvent was removed under reduced pressure and a gray powder was obtained. Yield, 60%. ¹H NMR (300 MHz, [D₆]DMSO, δ (ppm)): 6.3 (6H, s), 9.8 (2H, d), 9.2 (2H, m), 8.4 (2H, m), 8.0 (m, 2H), 7.4 (d, 2H). ESI-MS (in MeOH, *m/z*): 541.13 [M]⁺. RuC₂₆H₂₀N₄OCl: C, 57.64; H, 3.67; N, 10.38; Found: C, 57.67; H, 3.69; N, 10.35.

Synthesis of [Ru(η⁶-C₆H₆)(p-CFPIP)Cl]²⁺ (**2**)

The complex was synthesized in the same way as has been described for [Ru(η⁶-C₆H₆)(p-MOPIP)Cl]⁺ with p-MOPIP (0.058 g, 0.17 mmol) in place of p-CFPIP. Yield, 53%. ¹H NMR (300 MHz, [D₆]DMSO, δ (ppm)): 6.3 (6H, s), 9.8 (2H, d), 9.2 (2H, m), 8.6 (2H, m), 8.1 (m, 2H), 7.9 (d, 2H). ESI-MS (in MeOH, *m/z*): 579.00 [M - H]⁺. RuC₂₆H₁₇N₄F₃Cl: C, 53.85; H, 2.95; N, 9.68; Found: C, 53.88; H, 2.93; N, 9.67.

Absorption spectra studies

Absorption spectra titrations were carried out at room temperature to determine the binding affinity between DNA and complex. Initially, 3 mL solutions of the blank buffer and the ruthenium complex sample (10 μM) were placed in the reference and sample cuvettes (1.0 cm path length), respectively, and then the first spectrum was recorded in the range of 200–600 nm. During the titration, an aliquot (1–10 μL) of buffered DNA solution was added to each cuvette to eliminate the absorbance of DNA itself, and the solutions were mixed by repeated inversion. Complex–DNA solutions were incubated for 5 min before absorption spectra were recorded. The titration processes were repeated until there was no change in the spectra for four titrations at least, indicating binding saturation had been achieved. The changes in the metal complex concentration due to dilution at the end of each titration were negligible.

Gel mobility shift assay

Oligonucleotides at a concentration of 10 μM were annealed by heating in a 10 mM Tris/1 mM EDTA buffer containing 100 mM KCl (pH 8.0) to 95 $^{\circ}\text{C}$ for 10 min followed by cooling to room temperature. A stock solution (2 μL) of the metal complex was added. The reaction mixture was incubated at room temperature for 1 h and loaded onto a native 12% acrylamide vertical gel (1/19 bisacrylamide) in Tris borate EDTA (TBE) buffer, supplemented with 20 mM KCl. The reaction was terminated by addition of 8 μL of gel loading buffer (30% glycerol, 0.1% bromophenol blue, 0.1% xylene cyanol), and the subsequent solution (10 μL) was analyzed on a 12% native PAGE (the gel was prerun for 30 min). Electrophoresis was performed at 4 $^{\circ}\text{C}$ in TBE buffer (pH 8.3) containing 20 mM KCl for 15 h. The gels were dried and visualized with a Phosphor Imager.

Circular dichroism measurements

Circular dichroism (CD) spectra were measured on a Jasco J-810 spectropolarimeter. The CD titration procedure is described as follows: 1.0 μL Ru^{II} (1 mM) complex was added sequentially to solutions containing G-quadruplex DNA (2.0 μM). All solutions were mixed thoroughly and allowed to equilibrate for 5 min before data collection. The titration process was repeated several times until no change was observed. It indicated that binding saturation was achieved. For each sample, the spectrum was scanned at least three times and accumulated over the wavelength range of 200–350 nm at a temperature of 25 $^{\circ}\text{C}$. The instrument was flushed continuously with pure evaporated nitrogen throughout the experiment. The scan of the buffer alone was subtracted from the average scan for each sample.

Fluorescence resonance energy transfer (FRET) studies

The fluorescent labeled oligonucleotide, F21T (5'- FAM-G3[T2AG3]3-TAMRA-3', FAM: 6-carboxyfluorescein, TAMRA: 6-carboxy-tetramethylrhodamine) used as the FRET probes were diluted in Tris-HCl buffer (10 mM, pH 7.4) containing 60 mM KCl and then annealed by heating to 92 $^{\circ}\text{C}$ for 5 min, followed by cooling slowly to room temperature overnight. Fluorescence melting curves were determined with a Bio-Rad iQ5

real time PCR detection system, using a total reaction volume of 25 μL , with 1 μM of labeled oligonucleotide and different concentrations of complexes in Tris-HCl buffer (10 mM, pH 7.4) containing 60 mM KCl. A constant temperature was maintained for 30 s prior to each reading to ensure a stable value. Final analysis of the data was carried out using Origin 7.5 (OriginLab Corp.).

PCR stop assay

The oligonucleotide HTG21 (5'-G3(T2AG3)3-3') and the corresponding complementary sequence (HTG21rev, ATCGCT2CTCGTC3TA2C2) were used here. The reactions were performed in 1 \times PCR buffer, containing 10 pmol of each oligonucleotide, 0.16 mM dNTP, 2.5 U Taq polymerase, and different concentrations of complexes. Reaction mixtures were incubated in a thermocycler with the following cycling conditions: 94 $^{\circ}\text{C}$ for 3 min, followed by 30 cycles of 94 $^{\circ}\text{C}$ for 30 s, 58 $^{\circ}\text{C}$ for 30 s, and 72 $^{\circ}\text{C}$ for 30 s. PCR products were then analysed on 15% nondenaturing polyacrylamide gels in 1 \times TBE and silver stained.

TRAP assay

Telomerase extract was prepared from HeLa cells. The TRAP assay was performed using a modified procedure.^{36–38} PCR was performed at a final reaction volume of 50 μL , composed of a 45 μL reaction mix containing 20 mM Tris-HCl (pH 8.0), 50 μM deoxynucleotide triphosphates, 1.5 mM MgCl₂, 63 mM KCl, 1 mM EGTA, 0.005% Tween 20, 20 $\mu\text{g mL}^{-1}$ BSA, 3.5 pmol of primer HTG21 (5'-G3(T2AG3)3-3'), 18 pmol of primer TS (5'-A2TC2GTTCGAGCAGAGT2-3'), 22.5 pmol of primer CXext (5'-GTGC3T2AC3T2AC3T2AC3TA2-3'), 7.5 pmol of primer NT (5'-ATCGCT2CTCG2C2TTT4-3'), 0.01 amol of TSNT internal control (5'-A2TC2GTTCGAGCAGAGT2AA4AG2C2GAGA2GCGAT-3'), 2.5 U of Taq DNA polymerase, and 100 ng of telomerase. Compounds or distilled water were added under a volume of 5 μL . PCR was performed in an Eppendorf Master cycler equipped with a hot lid and incubated for 30 min at 30 $^{\circ}\text{C}$, followed by 92 $^{\circ}\text{C}$ for 30 s, 52 $^{\circ}\text{C}$ for 30 s, and 72 $^{\circ}\text{C}$ for 30 s for 30 cycles. After amplification, 8 μL of loading buffer (containing 5 \times Tris-Borate-EDTA buffer (TBE buffer), 0.2% bromophenol blue, and 0.2% xylene cyanol) was added to the reaction. A 15 μL aliquot was loaded onto a 16% non-denaturing acrylamide gel (19:1) in 1 \times TBE buffer and electrophoresed at 200 V for 1 h. Gels were fixed and then stained with AgNO₃.

Preparation of Ru complex-promoted G-quadruplex–hemin DNAzyme

An equal volume of Ru complexes solution (in water) was added to the DNA solutions (20 mM DNA, 10 mM Tris-HCl, 100 μM EDTA, pH = 8.00), allowing the DNA strands to form the G-quadruplex structure in 40 min. Then an equal volume of hemin (in DMSO) was dissolved in the above G-quadruplex solutions and kept for 2 h at room temperature to form the DNAzymes. Subsequently, 180 μL of 296 μM TMB–1.76 mM H₂O₂ solution was added as the substrate of above 20 μL peroxidatic DNAzyme system. The mixture was kept for 1.5 h at room temperature, different colors were observed with the naked eye and the photograph of the mixture was taken with a digital camera.

Cell culture

Cells were cultured in RPMI 1640 medium supplemented with 10% heat inactivated fetal bovine serum, 100 $\mu\text{g mL}^{-1}$ penicillin, and 100 $\mu\text{g mL}^{-1}$ streptomycin. Cells were maintained at 37 °C in a 5% CO_2 incubator, and the media were changed twice weekly.

MTT assay

Cell viability was determined by measuring the ability of cells to transform MTT (3-(4,5-dimethyl-2-thiazolyl)-2,5-diphenyl tetrazolium bromide) to a purple formazan dye.³⁹ Cells were grown in a RPMI 1640 medium supplemented with 10% fetal calf serum, 100 $\mu\text{g mL}^{-1}$ penicillin and 100 $\mu\text{g mL}^{-1}$ streptomycin. They were incubated at 37 °C in a humidified incubator with 5% CO_2 and 95% air. Cells at the exponential growth stage were diluted to 5×10^3 cells mL^{-1} with RPMI 1640, and then seeded in 96-well culture clusters (Costar) at a volume of 100 μL per cell, and incubated for 24 h at 37 °C in 5% CO_2 . Then the cells were treated with various concentrations of complexes, including 5, 10, 25, 50, 75, 100, 150 and 200 $\mu\text{mol L}^{-1}$, the media control and the drug-free control were set at the same time. After incubation of cells for up to 48 h, 100 μL of MTT (5 mg mL^{-1}) solution was added in each cell. After a further period of incubation (4 h at 37 °C in 5% CO_2), each cell was added in 100 μL cell lysate. After 12 h at 37 °C, plates were read on a microplate-reader at a wavelength of 570 nm (the absorbance of the complexes at this wavelength can be neglected^{40–42}). The percentage growth inhibitory rate of treated cells was calculated by $(A_{\text{tested}} - A_{\text{media control}})/(A_{\text{drug-free control}} - A_{\text{media control}}) \times 100\%$, where A is the mean value calculated using the data from three replicate tests. The IC_{50} values were determined by plotting the percentage viability *versus* concentration on a logarithmic graph and reading off the concentration at which 50% of cells were viable relative to the control.

Results and discussion

The binding affinity by absorption spectra

Absorption spectra titrations were performed to determine the binding affinity of complexes to HTG21. The changes in the spectral profiles during titration were shown in Fig. 2 (CT-DNA in Fig. S1, ESI†). The hypochromisms ($H\%$), defined as $H\% = 100\% \cdot (A_{\text{free}} - A_{\text{bound}})/A_{\text{free}}$, of MLCT bands of complexes **1** and **2**, were calculated as about 19.2% and 18.5%, respectively. When CT-DNA was added to the same buffered solution, the hypochromisms ($H\%$) was 12.5% and 23.6%, respectively. In order to compare the DNA-binding affinities of the two complexes quantitatively, their intrinsic DNA-binding constants K_b were obtained by monitoring the changes of the MLCT absorbance of both complexes according to Eq. (1)^{43–45} (see ESI†). The intrinsic binding constants K_b (HTG21) of complexes **1** and **2** were $3.87 \times 10^5 \text{ M}^{-1}$ and $2.14 \times 10^5 \text{ M}^{-1}$, respectively, from the decay of the absorbance (Table S1, ESI†). The binding constant K_b of complex **1** is larger than that of complex **2**. However, when compared to CT-DNA, the K_b order of complex **1** and complex **2** was reversed (Fig. S1, ESI†). It indicated that complex **1** bound to the HTG21 more tightly than did complex **2**. Upon comparison of **1** and **2**, compound **1** appeared to be more selective for HTG21 than CT-DNA.

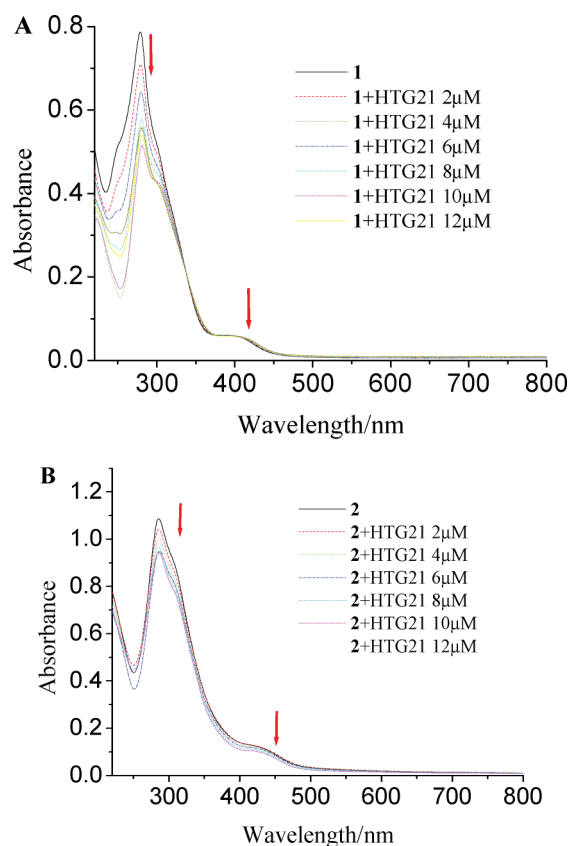


Fig. 2 Absorption spectra of complexes **1** (A) and **2** (B) in buffer with increasing amounts of G-quadruplex. $[\text{Ru}] = 10.0 \mu\text{M}$, $[\text{DNA}] = 0\text{--}12 \mu\text{M}$ from top to bottom. Arrows refer to the change in absorbance upon increasing the concentration of DNA.

Gel mobility shift assay

By employing a native PAGE assay, we examined the ability of the complexes to assemble intermolecular G-quadruplexes from the oligonucleotide HTG21, which contains four repeats of the human telomeric sequence and hence has the potential to form both parallel and antiparallel G-quadruplex structures, in dimeric (D) and tetrameric (T) forms (Fig. 3).^{46–48} For example, Hurley *et al.* have reported the DNA oligomer d(TTAGGG)₄ (HT4) was incubated with increasing concentrations of the three porphyrins; we observed an increased amount of dimers (D) in the presence of TMPyP3, TMPyP4 and only tetrameric (T) in the presence of TMPyP3. Che *et al.* has also proven the ability of the complexes to assemble intermolecular G-quadruplexes from the oligonucleotide which contains two tandem human telomeric sequences and can associate into antiparallel and parallel G-quadruplexes, in dimeric (D) and tetrameric (T) forms. Under the buffer conditions used in the experiment (10 mM Tris, 1 mM EDTA, pH 8.0) and in the absence of complexes, gel mobility shift assays revealed that there was no formation of G-quadruplex structure and only the band corresponding to the monomer (M) could be observed (Fig. 4). When HTG21 was incubated with increasing concentrations of complexes, we observed an increased amount of dimers (D) in the presence of **1** and **2**, in particular for treatment of HTG21 oligonucleotide with complexes **1** and **2** at concentrations up to 30 μM , the appearance of new bands with

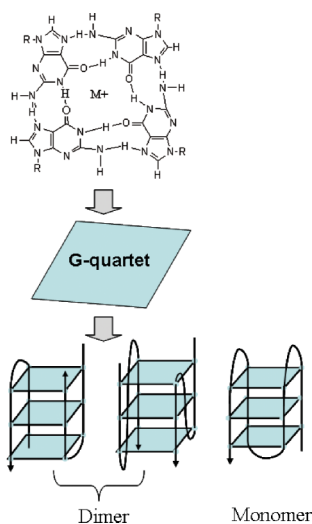


Fig. 3 The quadruplex: tetrameric, dimeric and monomeric G-quadruplex composed of three G-quartets.

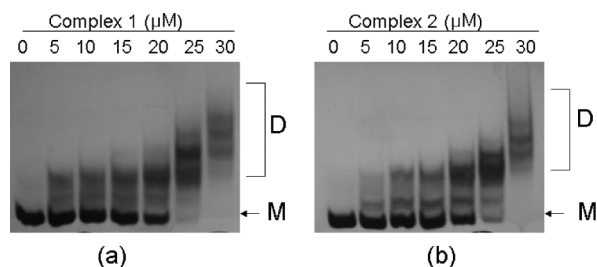


Fig. 4 Effect of complex **1** (a) and **2** (b) on the assembly of the HTG21 structure illustrated by native PAGE analysis. Ruthenium complexes at the indicated concentrations were incubated with HTG21 (10 μM) at 20 $^{\circ}\text{C}$ in a buffer containing 10 mM Tris, 1 mM EDTA, pH 8.0. Major bands were identified as monomer (M), dimer (D).

reduced mobility, corresponding to the D G-quadruplex structures were most conspicuous. These bands were also observed when oligonucleotide HTG21 was incubated in K^+ containing Tris buffer (10 mM Tris, 1 mM EDTA, 100 mM KCl, pH 8.0) (Fig. S2, ESI †). Compared to in the absence of K^+ buffer, the D G-quadruplex structures bands were not obvious until the concentration of **1** and **2** reached 35 μM . The results showed that in the presence of potassium ions or not, complexes **1** and **2** were able to induce HTG21 oligonucleotide to form D G-quadruplex structures.

Circular dichroic spectral studies

Circular dichroism (CD) spectroscopy was used to characterize the solution conformations of HTG21. Without any metal cations, the CD spectra of HTG21 at room temperature exhibited a negative band centered at 235 nm, a major positive band at 257 nm, which probably corresponded to the signal of the random coil HTG21 (characterized by a positive peak at 257 nm).^{49,50} Upon addition of complex **1** to HTG21 aqueous solution (Fig. 5), a significant change in the CD spectrum was observed. With the increase of **1** from 1 μM to 3 μM , the maximum at 257 nm was gradually suppressed and shifted to 249 nm, while a major negative band at about 270 and a major positive band at 295 nm started to appear. We thought that as the concentration continued

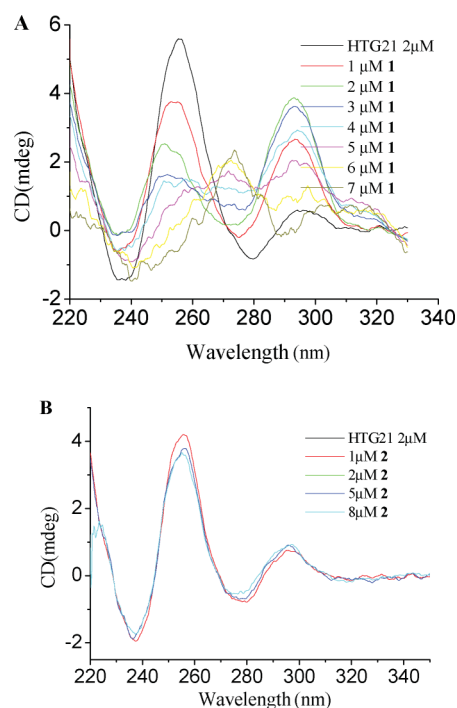


Fig. 5 CD spectra of HTG21 acquired at 20 $^{\circ}\text{C}$ in the absence or presence of different concentrations of **1** (A) and **2** (B). All experiments were carried out in 10 mM Tris-HCl, pH 7.4. The HTG21 concentration was 2 μM .

to increase, the CD spectrum of this new DNA conformation would appear similar to the antiparallel G-quadruplexes described in previous studies, where the major positive band was usually observed around 295 nm with a negative band at 265 nm and a smaller positive band at 246 nm. However, a strange phenomenon was found in the CD spectrum. A major positive band at 295 nm started to wane and a new positive band gradually appeared. The addition of complex **2** did not induce obvious changes in CD spectra. This interesting phenomenon occurs probably because HTG21 DNA is a quadruplex, there are also several different folding motifs possible to create a quadruplex as alluded to in Fig. 3, and another point is closely related to the different ligands. The structures of G-quadruplex were also investigated in the Na^+ or K^+ buffer solution. Upon addition of complexes **1** and **2** to HTG21 in Na^+ or K^+ buffer solution, the CD spectrum exhibited a maxima-minima pattern, similar but not identical to the spectrum in Na^+ or K^+ without addition of the two complexes (Fig. S3 and S4, ESI †), which implied that the conformation of the G-quadruplex was stabilized by Na^+ or K^+ , and **1** or **2** could not change the conformation of the G-quadruplex at high ionic strength. For ssDNA, when complex **2** was added, the bands at about 280 nm and 250 nm significantly decreased and reached saturation. However, upon addition of complex **1**, no obvious spectral changes were observed under the same conditions (in Fig. S5, ESI †). Upon interacting complex **2** with CT DNA ([DNA]/[Ru] = 1 : 1), we find the maximum at 275 nm with a slightly higher intensity and a new negative band at about 290 nm, suggesting the conformation of CT DNA has been changed. In contrast to **2**, the CD spectrum of DNA in the presence of complex **1** showed no change under the same experimental conditions (in Fig. S6, ESI †). These data clearly suggest that both complexes, especially **1**, strongly and selectively

Table 1 ΔT_m values at various concentrations of **1** and **2**, F21T (1 μM)

Complexes (μM)	ΔT_m ($^\circ\text{C}$)	
	1	2
1	15	9
2.5	22	17
5	27	21

interact with G-quadruplex DNA over ssDNA and CT-DNA. The results reveal that the different ligands of complexes **1** and **2** are related to the mode of DNA binding, and **2** can bind more strongly to CT DNA than complex **1**.

Thermodynamic stabilization of the telomeric G-quadruplex by complexes **1** and **2**

FRET (fluorescence resonance energy transfer) can be used as a convenient method to monitor the 3'-to-5'-end distance.^{51,52} In this paper, we used a FRET melting assay to investigate the binding abilities of **1** and **2** to G-quadruplex DNA F21T (sequence: FAM-G3[T2AG3]3-TAMRA, mimicking the human telomeric repeat).⁵³ As shown in Fig. 6, in the absence of any Ru^{II} complex, the DNA melting temperature (T_m) of F21T in Tris/KCl buffer was 48 $^\circ\text{C}$. Upon treatment of the F21T (1 μM) with concentration ratios $[\text{RuI}]/[\text{DNA}] = 1:1, 2.5:1$ and $5:1$, the highest T_m deviation $[\Delta T_m$ (change in DNA melting temperature) = 27 $^\circ\text{C}$] was found with **1**. When compared to **1**, complex **2** ($\Delta T_m = 9, 17, 21$ $^\circ\text{C}$, respectively) is not a very effective quadruplex-DNA stabilizer (Table 1). This is consistent with the results of the absorption titration studies showing that **1** has the higher K value [$3.87 \times 10^5 \text{ M}^{-1}$]. The results indicated that both complexes can stabilize G-quadruplex DNA and that complex **1** affected the stability of the G-quadruplex more than complex **2**. The difference may originate from the different DNA-binding affinity. The mechanism is not yet clear, however the ligand of the Ru^{II} complex plays a key role in stabilization. It was found that, in relation to binding abilities, the electron withdrawing group trifluoromethyl was inferior to the electron donor methoxy, consistent with circular dichroism spectral studies.

Inhibition of amplification of HTG21 by Ru complexes **1** and **2**

In order to further evaluate the ability of complexes **1** and **2** to stabilize G-quadruplex DNA, a polymerase chain reaction (PCR) stop assay was used to ascertain whether complexes bound to the test oligomer (5'-G3(T2AG3)3-3') and stabilized the G-quadruplex structure.⁵⁴⁻⁵⁶ In the presence of complexes **1** or **2**, the template sequence HTG21 was induced into a G-quadruplex structure that blocked the hybridization with a complementary primer sequence. In that case, 5' to 3' primer extension by DNA Taq polymerase was arrested and the final double-stranded DNA PCR product could not be detected.^{55,57} The inhibitory effect of **1** was clearly enhanced as the concentration increased from 0.2 to 5.0 μM , with no PCR product detected at 5.0 μM (Fig. 7, left). However, even if the concentration of **2** was allowed to exceed 7.5 μM , **2** could not completely inhibit the appearance of the PCR product, which further indicates that complex **1** is a better G-quadruplex binder.

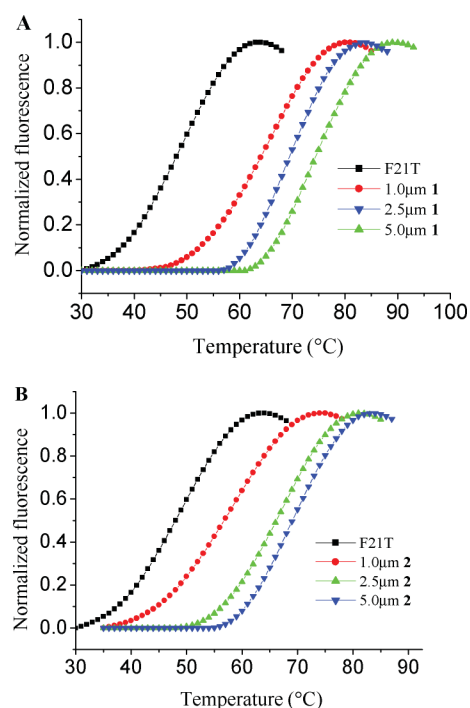


Fig. 6 (A) FRET-melting curves obtained with F21T (1 μM) alone (■) and with **1** = 1.0 μM to 5 μM . (B) FRET-melting curves obtained with F21T (1 μM) alone (■) and with **2** = 1.0 μM to 5 μM .

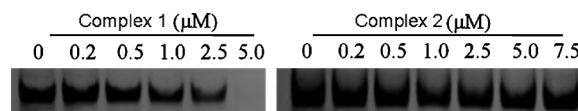


Fig. 7 Effect of complexes **1** (0–5.0 μM , left) and **2** (0–7.5 μM , right) on the hybridization of HTG21 in the PCR-stop assay.

TRAP assay

On the basis of the obtained results, it appeared to be of interest to compare the ability of the two arene ruthenium complexes to inhibit the enzyme telomerase. For this, a modified version of the telomeric repeat amplification protocol (TRAP) assay was performed (Fig. 8). In this experiment, solutions of complexes **1** and **2** were added to a telomerase reaction mixture containing extracts from HeLa cells, which express high levels of telomerase activity. Fig. 8 showed the *in vitro* inhibitory effect of complex **1** towards telomerase studied in a dose-dependent manner and the number of bands clearly decrease with respect to the control, at drug concentrations in the range of 1–16 μM . In contrast, no complete inhibition was observed in the presence of **2**, even at 16 μM (Fig. 8). The two ruthenium complexes tested led to an inhibition of the enzyme telomerase, but there were great differences in the extent of inhibition. The results clearly revealed that the telomerase inhibitory properties of **1** were significantly greater, which is in accordance with the experimental data from the thermodynamic stability study and the PCR stop assay.

Visual detection of G-quadruplex structures by Ru complex

Although certain kinds of G-rich sequences have been demonstrated to form G-quadruplex structures readily at physiological

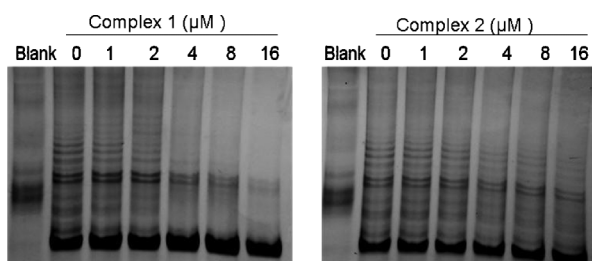


Fig. 8 The influence of $[\text{Ru}(\eta^6\text{-C}_6\text{H}_6)(\text{p-MOPIP})\text{Cl}]^+$ (**1**) and $[\text{Ru}(\eta^6\text{-C}_6\text{H}_6)(\text{p-CFPIP})\text{Cl}]^+$ (**2**) on the telomere activity of HeLa.

concentrations of Na^+ and K^+ *in vitro*,^{58–61} the existence of G-quadruplex structures *in vivo* is still controversial.^{62,63} The lack of direct evidence for this quadruplex structure in living cells is a serious obstacle to determining its function. Thus, detecting G-quadruplex structures has great significance for cell proliferation, cancer research, and drug development. Here we report a facile and visual approach to detect G-quadruplexes with the naked eye.

It is well known that most G-quadruplex DNA can be effectively formed by K^+ , and G-quadruplexes have the ability to bind with hemin to form peroxidase-like DNAzymes. It is proven that in the presence of the DNAzymes, H_2O_2 -mediated oxidation of TMB (3,3',5,5'-tetramethylbenzidine) could be sharply accelerated and the color change is very sensitive and easy to identify. The design is based on this principle. As shown in Fig. 9, in the presence of complex **1** or **2**, HTG21 can also fold into a G-quadruplex, and such a quadruplex structure is able to bind hemin to form the hemin–G-quadruplex DNAzyme that catalyzes the H_2O_2 -mediated oxidation of colorless TMB to the blue product, as well as control K^+ . But for complex **1** with double strands of CT-DNA, the solution remains colorless. The reason is obvious, because CT-DNA cannot form the G-quadruplex structure. Furthermore, under the same conditions, when using the ligands p-MOPIP (**L1**) and p-CFPIP (**L2**) the solution does not change colour at all (Fig. S7, ESI†).

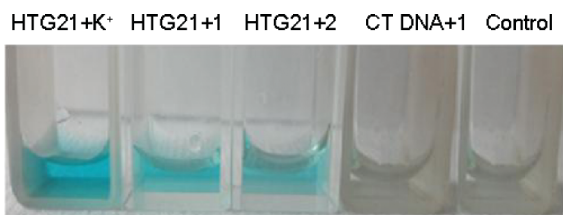


Fig. 9 Characterization of the DNAzyme functions of HTG21 DNA and CT-DNA in the presence of 500 nM K^+ , 500 nM **1** and 500 nM **2** in the TMB– H_2O_2 system. Conditions: TMB, 266 mM in Tris–MES buffer (25 mM MES, pH = 5.10); H_2O_2 , 794 mM; DNA, 500 nM; hemin, 500 nM.

In vitro cytotoxicity

To explore the antitumor potential of the Ru^{II} complexes, HepG2 (human hepatocellular liver carcinoma), HeLa (human cervical cancer), A549 (human lung carcinoma), SW620 (colorectal adenocarcinoma) and NIH/3T3 (mouse embryonic fibroblast) cells were treated with varying concentrations of Ru^{II} complexes for 48 h, and cell viability was determined by the MTT assay. Table S2, ESI† shows the IC_{50} values of two arene ruthenium complexes

and cisplatin. The tested cancer cells, especially the HeLa cells, were susceptible to the complexes. It is particularly interesting that the antiproliferative activities of complex **1** were higher than those of **2**, as evidenced by the lower IC_{50} values. Notably, complex **1** exhibited a broad spectrum of inhibition on human cancer cells, with IC_{50} values ranging from 8.70 to 35.72 μM , indicating the higher cytotoxic effects of complex **1** on cancer cells. It is also worth noting that **1** shows a distinct preference for HeLa cells (approximately as potent as cisplatin towards this cell line). In addition, we also detected the antiproliferative activity of the Ru^{II} complexes on the mouse embryonic fibroblast cell line NIH/3T3. Generally, this series of complexes inhibited the growth of cancer cell lines better than normal cells, suggesting the Ru^{II} complexes were much less toxic towards normal cells, with IC_{50} values of 48.37 μM and greater than 100 μM , which were significantly higher than those of cisplatin (19.72 μM). The results showed that complex **1** exhibited quite potent antitumor activities and the greatest inhibitory selectivity against cancer cell lines.

Conclusions

In conclusion, two η^6 -arene ruthenium with 1,10-phenanthroline-derived ligands have been prepared and interacted with G-quadruplex DNA. The results showed that complex **1** bound to the DNA more tightly than did complex **2**. Complex **1** is a potent telomerase inhibitor and a very good G-quadruplex DNA stabilizer that can increase the T_m value of G quadruplexes by 9–27 °C. Successful quadruplex DNA binders should not only interact strongly with their target but also exhibit high selectivity for quadruplex *versus* duplex DNA. In this work, more importantly, complex **1** could significantly stabilize and induce intramolecular G-quadruplex structural transitions and has made a significant choice of G-quadruplex DNA. The visual observation of G-quadruplexes has also been successfully used in investigating the one-stranded telomeric and double-stranded calf thymus DNA. *In vitro* cytotoxicity studies showed complex **1** exhibited quite potent antitumor activities and the greatest inhibitory selectivity against cancer cell lines. The electron-withdrawing or electron-donating properties of substituents were determined to be critical for interaction. Complex **1** was observed to have a greater ability to interact with quadruplex DNA as it contains a ligand with a pendant $-\text{OCH}_3$ functional group, which may be involved in H-bonding interactions with the guanine in the external tetrad of G-quadruplex DNA. The PIP ligands might be partially inserted into the plane of G-quadruplex DNA and the η^6 -arene ligand might interact with G-quadruplex DNA by π – π stacking. Although the details of the binding modes of these complexes with the G-quadruplex and the structure of the G-quadruplex are not clear yet, in our research we can draw the following conclusions: (1) η^6 -arene ruthenium complexes exert a stabilization effect towards the G-quadruplex structure and show good selectivity between dsDNA and G-quadruplexes. The changes in microenvironment ($-\text{OCH}_3$, $-\text{CF}_3$) in the complexes affects the binding capacity. (2) Complexes can induce changes in G-quadruplex DNA conformation and the structures of complexes can also affect the changes of G-quadruplex DNA. (3) The complexes have the ability to stabilize G-quadruplex DNA and induce the transformation of G-quadruplex DNA conformation, which closely relates to the inhibition of telomerase activity and *in vitro* antitumor activity.

We speculate telomerase is the target of the antitumor activity of these complexes.

Acknowledgements

This work was supported by the National Natural Science Foundation of China (20871056), the Planned Item of Science and Technology of Guangdong Province (c1011220800060), the 211 project grant of Jinan University, and “the Fundamental Research Funds for the Central Universities”.

References

- 1 E. H. Blackburn, *Annu. Rev. Biochem.*, 1984, **53**, 163–194.
- 2 E. H. Blackburn, *J. Biol. Chem.*, 1990, **265**, 5919–5921.
- 3 R. McElligott and R. J. Wellinger, *EMBO J.*, 1997, **16**, 3705–3714.
- 4 W. E. Wright, V. M. Tesmer, K. E. Huffman, S. D. Levene and J. W. Shay, *Genes Dev.*, 1997, **11**, 2801–2809.
- 5 K. E. Huffman, S. D. Levene, V. M. Tesmer, J. W. Shay and W. E. Wright, *J. Biol. Chem.*, 2000, **275**, 19719–19722.
- 6 N. W. Kim, M. A. Piatyszek, K. R. Prowse, C. B. Harley, M. D. West, P. L. Ho, G. M. Coviello, W. E. Wright, S. L. Weinrich and J. W. Shay, *Science*, 1994, **266**, 2011–2015.
- 7 C. M. Counter, H. W. Hirte, S. Bacchetti and C. B. Harley, *Proc. Natl. Acad. Sci. U. S. A.*, 1994, **91**, 2900–2904.
- 8 E. Hiyama, L. Gollahon, T. Kataoka, K. Kuroi, T. Yokoyama, A. F. Gazdar, K. Hiyama, M. A. Piatyszek and J. W. Shay, *J. Natl. Cancer Inst.*, 1996, **88**, 116–122.
- 9 E. Hiyama, T. Yokoyama, N. Tatsumoto, K. Hiyama, Y. Imamura, Y. Murakami, T. Kodama, M. A. Piatyszek, J. W. Shay and Y. Matsuura, *Cancer Res.*, 1995, **55**, 3258–3262.
- 10 K. Hiyama, E. Hiyama, S. Ishioka, M. Yamakido, K. Inai, A. F. Gazdar, M. A. Piatyszek and J. W. Shay, *J. Natl. Cancer Inst.*, 1995, **87**, 895.
- 11 T. M. Fletcher, *Expert Opin. Ther. Targets*, 2005, **9**, 457–469.
- 12 B. Herbert, A. E. Pitts, S. I. Baker, S. E. Hamilton, W. E. Wright, J. W. Shay and D. R. Corey, *Proc. Natl. Acad. Sci. U. S. A.*, 1999, **96**, 14276–14281.
- 13 S. Neidle and G. Parkinson, *Nat. Rev. Drug Discovery*, 2002, **1**, 383–393.
- 14 J. L. Mergny, J. F. Riou, P. Mailliet, M. P. Teulade-Fichou and E. Gilson, *Nucleic Acids Res.*, 2002, **30**, 839–865.
- 15 E. M. Rezler, D. J. Bearss and L. H. Hurley, *Curr. Opin. Pharmacol.*, 2002, **2**, 415–423.
- 16 A. De Cian, L. Lacroix, C. Douarre, N. Temime-Smaali, C. Trentesaux, J. F. Riou and J. L. Mergny, *Biochimie*, 2008, **90**, 131–155.
- 17 J. Sun, Y. An, L. Zhang, H.-Y. Chen, Y. Han, Y.-J. Wang, Z.-W. Mao and L.-N. Ji, *J. Inorg. Biochem.*, 2011, **105**, 149–154.
- 18 S. Shi, X. Geng, J. Zhao, T. Yao, C. Wang, D. Yang, L. Zheng and L. Ji, *Biochimie*, 2008, **92**, 370–377.
- 19 N. V. Anantha, M. Azam and R. D. Sheardy, *Biochemistry*, 1998, **37**, 2709–2714.
- 20 J. E. Reed, A. A. Arnal, S. Neidle and R. Vilar, *J. Am. Chem. Soc.*, 2006, **128**, 5992–5993.
- 21 J. E. Reed, S. Neidle and R. Vilar, *Chem. Commun.*, 2007, 4366–4368.
- 22 R. T. Wheelhouse, D. Sun, H. Han, F. X. Han and L. H. Hurley, *J. Am. Chem. Soc.*, 1998, **120**, 3261–3262.
- 23 K. Gehring, J.-L. Leroy and M. Gueron, *Nature*, 1993, **363**, 561–565.
- 24 Y. Wang and D. J. Patel, *Structure*, 1993, **1**, 263–282.
- 25 G. N. Parkinson, M. P. H. Lee and S. Neidle, *Nature*, 2002, **417**, 876–880.
- 26 S. Rickling, L. Ghisdavu, F. Pierard, P. Gerbaux, M. Surin, P. Murat, E. Defranco, C. Moucheron and A. Kirsch-De Mesmaeker, *Chem.-Eur. J.*, 2010, **16**, 3951–3961.
- 27 D. Monchaud, C. Allain, H. Bertrand, N. Smargiasso, F. Rosu, V. Gabelica, A. De Cian, J. L. Mergny and M. P. Teulade-Fichou, *Biochimie*, 2008, **90**, 1207–1223.
- 28 J. E. Redman, *Methods*, 2007, **43**, 302–312.
- 29 C. R. Cantor, M. M. Warshaw and H. Shapiro, *Biopolymers*, 1970, **9**, 1059–1077.
- 30 J. Marmur and P. Doty, *J. Mol. Biol.*, 1961, **3**, 585–594.
- 31 W. Paw and R. Eisenberg, *Inorg. Chem.*, 1997, **36**, 2287–2293.
- 32 M. A. Bennett and A. K. Smith, *J. Chem. Soc., Dalton Trans.*, 1974, 233–241.
- 33 M. A. Bennett and T. W. Matheson, *J. Organomet. Chem.*, 1979, **175**, 87–93.
- 34 C. M. Dupureur and J. K. Barton, *Inorg. Chem.*, 1997, **36**, 33–43.
- 35 J. Canivet, L. Karmazin-Brelot and G. Suss-Fink, *J. Organomet. Chem.*, 2005, **690**, 3202–3211.
- 36 N. W. Kim, M. A. Piatyszek, K. R. Prowse, C. B. Harley, M. D. West, P. L. Ho, G. M. Coviello, W. E. Wright, S. L. Weinrich and J. W. Shay, *Science*, 1994, **266**, 2011.
- 37 N. W. Kim and F. Wu, *Nucleic Acids Res.*, 1997, **25**, 2595.
- 38 G. Krupp, K. Kühne, S. Tamm, W. Klapper, K. Heidorn, A. Rott and R. Parwaresch, *Nucleic Acids Res.*, 1997, **25**, 919.
- 39 O. Morgan, S. Wang, S. A. Bae, R. J. Morgan, A. D. Baker, T. C. Streckas and R. Engel, *J. Chem. Soc., Dalton Trans.*, 1997, 3773–3776.
- 40 S. A. Kurzeev, A. S. Vilesov, T. V. Fedorova, E. V. Stepanova, O. V. Koroleva, C. Bukh, M. J. Bjerrum, I. V. Kurnikov and A. D. Ryabov, *Biochemistry*, 2009, **48**, 4519–4527.
- 41 A. H. Velders, H. Kooijman, A. L. Spek, J. G. Haasnoot, D. de Vos and J. Reedijk, *Inorg. Chem.*, 2000, **39**, 2966–2967.
- 42 B. P. Sullivan, D. J. Salmon and T. J. Meyer, *Inorg. Chem.*, 1978, **17**, 3334–3341.
- 43 S. R. Smith, G. A. Neyhart, W. A. Kalsbeck and H. H. Thorp, *New J. Chem.*, 1994, **18**, 397–406.
- 44 R. B. Nair, E. S. Teng, S. L. Kirkland and C. J. Murphy, *Inorg. Chem.*, 1998, **37**, 139–141.
- 45 M. T. Carter, M. Rodriguez and A. J. Bard, *J. Am. Chem. Soc.*, 1989, **111**, 8901–8911.
- 46 D.-L. Ma, C.-M. Che and S.-C. Yan, *J. Am. Chem. Soc.*, 2008, **131**, 1835–1846.
- 47 M.-P. Teulade-Fichou, C. Carrasco, L. Guittat, C. Bailly, P. Alberti, J.-L. Mergny, A. David, J.-M. Lehn and W. D. Wilson, *J. Am. Chem. Soc.*, 2003, **125**, 4732–4740.
- 48 H. Han, C. L. Cliff and L. H. Hurley, *Biochemistry*, 1999, **38**, 6981–6986.
- 49 E. M. Rezler, J. Seenisamy, S. Bashyam, M.-Y. Kim, E. White, W. D. Wilson and L. H. Hurley, *J. Am. Chem. Soc.*, 2005, **127**, 9439–9447.
- 50 D. P. N. Goncalves, R. Rodriguez, S. Balasubramanian and J. K. M. Sanders, *Chem. Commun.*, 2006, 4685–4687.
- 51 R. M. Clegg, A. I. H. Murchie, A. Zechel, C. Carlberg, S. Diekmann and D. M. J. Lilley, *Biochemistry*, 1992, **31**, 4846–4856.
- 52 T. J. Meade and J. F. Kayyem, *Angew. Chem., Int. Ed. Engl.*, 1995, **34**, 352–354.
- 53 J.-L. Mergny and J.-C. Maurizot, *ChemBioChem*, 2001, **2**, 124–132.
- 54 H. Han, L. H. Hurley and M. Salazar, *Nucleic Acids Res.*, 1999, **27**, 537–542.
- 55 T. Lemarteleur, D. Gomez, R. Paterski, E. Mandine, P. Mailliet and J. F. Riou, *Biochem. Biophys. Res. Commun.*, 2004, **323**, 802–808.
- 56 J. T. Wang, X. H. Zheng, Q. Xia, Z. W. Mao, L. N. Ji and K. Wang, *Dalton Trans.*, 2010, **39**, 7214–7216.
- 57 Y. J. Lu, T. M. Ou, J. H. Tan, J. Q. Hou, W. Y. Shao, D. Peng, N. Sun, X. D. Wang, W. B. Wu, X. Z. Bu, Z. S. Huang, D. L. Ma, K. Y. Wong and L. Q. Gu, *J. Med. Chem.*, 2008, **51**, 6381–6392.
- 58 L. Petraccone, J. O. Trent and J. B. Chaires, *J. Am. Chem. Soc.*, 2008, **130**, 16530–16532.
- 59 H.-Q. Yu, D. Miyoshi and N. Sugimoto, *J. Am. Chem. Soc.*, 2006, **128**, 15461–15468.
- 60 K. N. Luu, A. T. Phan, V. Kuryavyi, L. Lacroix and D. J. Patel, *J. Am. Chem. Soc.*, 2006, **128**, 9963–9970.
- 61 K. Shin-ya, K. Wierzba, K. Matsuo, T. Ohtani, Y. Yamada, K. Furihata, Y. Hayakawa and H. Seto, *J. Am. Chem. Soc.*, 2001, **123**, 1262–1263.
- 62 K. Paeschke, S. Juraneck, T. Simonsson, A. Hempel, D. Rhodes and H. J. Lipps, *Nat. Struct. Mol. Biol.*, 2008, **15**, 598–604.
- 63 K. Paeschke, T. Simonsson, J. Postberg, D. Rhodes and H. J. Lipps, *Nat. Struct. Mol. Biol.*, 2005, **12**, 847–854.